Apparent Subdiffusion Inherent to Single Particle Tracking

Douglas S. Martin, Martin B. Forstner, and Josef A. Käs
Center for Nonlinear Dynamics, University of Texas at Austin, Austin, Texas 78712 USA

ABSTRACT Subdiffusion and its causes in both in vivo and in vitro lipid membranes have become the focus of recent research. We report apparent subdiffusion, observed via single particle tracking (SPT), in a homogeneous system that only allows normal diffusion (a DMPC monolayer in the fluid state). The apparent subdiffusion arises from slight errors in finding the actual particle position due to noise inherent in all experimental SPT systems. A model is presented that corrects this artifact, and predicts the time scales after which the effect becomes negligible. The techniques and results presented in this paper should be of use in all SPT experiments studying normal and anomalous diffusion.

INTRODUCTION

Recent single particle tracking (SPT) experiments have found anomalous diffusion of membrane constituents on both cell and artificial membranes (Jacobson et al., 1995; Saxton and Jacobson, 1997; Schütz et al., 1997, 2000; Cherry et al., 1998; Smith et al., 1999; Collier et al., 2001). Anomalous diffusion of membrane proteins and lipids is exciting for two main reasons. Biologically, anomalous diffusion may be a method for cells to localize membrane receptors and control intramembrane signaling. Physically, non-Brownian diffusion indicates a breakdown of the central limit theorem, rarely observed in nature.

The SPT technique has been used in a large field of biophysical research to observe the lateral motions of lipids and proteins in both cell membranes, such as the plasma and nuclear membranes, and artificial membranes (for a comprehensive review, see Saxton and Jacobson, 1997). The technique is based on tracking the fluorescence or scattering signal of a nanoparticle bound to the molecule of interest (Gelles et al., 1988; Sheetz et al., 1989; Lee et al., 1991; Anderson et al., 1992; Ghosh and Webb, 1994; Schütz et al., 1997). In general, it involves a particle smaller than the diffraction limit that is only visible as an Airy disk on top of a noisy background. SPT relies on a signal strong enough that intensified cameras can detect the particle's diffraction peak with high spatial accuracy (typically tens of nanometers).

Normal diffusion of lipids and proteins is characterized by the mean square displacement (MSD) of the particle position growing linearly with respect to time, MSD $\sim t$. In anomalous subdiffusion, in contrast, the MSD of the motion grows as t^{α}, $\alpha < 1$, in the long time limit. Several models have been developed to explain anomalous diffusion on cell surfaces. They include diffusion with static obstacles such as fixed proteins (Saxton, 1994), cytoskeletal corrals where proteins are confined transiently to submicron corrals by interaction with the cytoskeleton beneath the membrane (Kusumi et al., 1993; Saxton, 1995), binding to obstacles (Saxton, 1996), and interaction with lipid rafts (Schütz et al., 2000).

We have extended the SPT technique to look at diffusion in the long time limit on Langmuir monolayers (Forstner et al., 2001), in part because it becomes easier to distinguish between scaling behaviors over long times. Interestingly, we found signatures of anomalous diffusion at short time scales, changing to normal diffusion at longer times. However, on homogeneous, fluid-phase dimyristoyl phosphatidylcholine (DMPC) monolayers, there is no underlying mechanism to give rise to anomalous diffusion. To resolve this discrepancy, we conducted simulations and created analytic representations of the motion to develop a model for the subdiffusion. Quantitative comparisons to data from our DMPC experiments show that this model explains the results and indeed is universal to SPT systems. We also provide guidelines for which timescales will remain unaffected in a noisy environment (always present in experimental systems).

Because many SPT systems have neither a large observation space nor long time tracks, observed subdiffusion may be the result of noise, and not any underlying mechanism; moreover, very reliable measurements are needed to determine scaling laws on short time experiments. The methods presented in this paper can help to make the measurements on short time systems more reliable, and, as such, are of more general interest.

The paper is organized in the following manner: in the next section, we present the model of how noise leads to subdiffusion, followed by the experimental and computational methods used to develop and test this model. We then present and discuss the results that confirm that apparent subdiffusion can arise simply from noise.

Submitted March 27, 2002 and accepted for publication May 31, 2002.

Address reprint requests to Douglas S. Martin, Center for Nonlinear Dynamics, Univ. of Texas at Austin, Austin, TX 78712. Tel.: 512-475-7647; Fax: 512-471-1558; E-mail: dmartin@chaos.ph.utexas.edu.

0006-3495/02/10/2109/09 $2.00

THEORY

We begin with an analytical method to explain how apparent subdiffusion occurs in noisy single-particle tracking.

The noise causes error in determining the particle position. This error changes the functional form of the mean square displacement, and hence any quantities that are derived from the MSD. In anomalous diffusion, the MSD is given by (Saxton and Jacobson, 1997)

$$\langle \mathbf{r}^2 \rangle = \mathrm{MSD}(\Delta t) = 4D\Delta t^{\alpha}, \tag{1}$$

where $\mathbf{r}(t)$ is the particle position at time t, D acts as the diffusion coefficient, α is the actual scaling exponent (note that we use the convention that α is the underlying anomalous diffusion coefficient and α_{ap} is the apparent exponent found in the SPT experiments), and Δt is the time lag between two positions. The averaging operation $\langle\ \rangle$ is over all positions separated by the same Δt. The standard method to test for anomalous diffusion is to find α through a linear fit to (Feder et al., 1996)

$$\log(\mathrm{MSD}(\Delta t)) = \alpha \log(\Delta t) + \log(4D), \tag{2}$$

because this fit converges more consistently than the variable power-law fit. The slope of this fit is the scaling exponent α, and the offset gives the diffusion coefficient D.

For the simpler case of Brownian motion in two dimensions, the mean square displacement is given by (Qian et al., 1991),

$$\mathrm{MSD}(\Delta t) = 4D\Delta t, \tag{3}$$

where D is the actual diffusion coefficient. When there is random error in the determination of the particle position, characterized by mean error σ, the MSD is calculated in the appendix, and given by (Eq. A8 and Dietrich et al., 2002),

$$\mathrm{MSD}(\Delta t) = 4D\Delta t + 2\sigma^2. \tag{4}$$

To find the diffusion coefficient, one standard method is to perform a linear fit to MSD(Δt). The slope is D and the intercept is $2\sigma^2$, although the intercept is generally discarded.

Now, however, the simple decomposition of log(MSD) given in Eq. 2 does not work. That is, finding the slope of $\log(4D\Delta t + 2\sigma^2)$ is more complex, and is worked out in detail in the Appendix (Eq. A10). This slope is the apparent scaling coefficient, α_{ap}, which is no longer constant even in Brownian motion with noise, and is given by

$$\alpha_{ap} = \frac{1}{1 + 2\sigma^2/4D\Delta t}. \tag{5}$$

The single parameter $2\sigma^2/4D$ determines how subdiffusive the motion will appear; the larger the parameter, the more subdiffusive the motion. For this reason, we use it to characterize $\alpha_{ap}(\Delta t)$. Note that this parameter has the units of seconds, when $2\sigma^2/4D = \Delta t$, $\alpha_{ap} = 0.67$.

This result is intuitively explained by comparing linear and logarithmic plots of the MSD with and without noise (MSD_n, MSD, respectively), as shown in Fig. 1, *a* and *b*. In the linear plot in Fig. 1 *a*, there is only a constant offset between MSD and MSD_n. In the logarithmic plot (Fig. 1 *b*), at short values of Δt, the difference between log(MSD) and $\log(\mathrm{MSD}_n)$ is large, whereas at long times, the difference is small. This means that the slope of $\log(\mathrm{MSD}_n)$, α_{ap}, must start out smaller than the slope of log(MSD), $\alpha = 1.0$, and

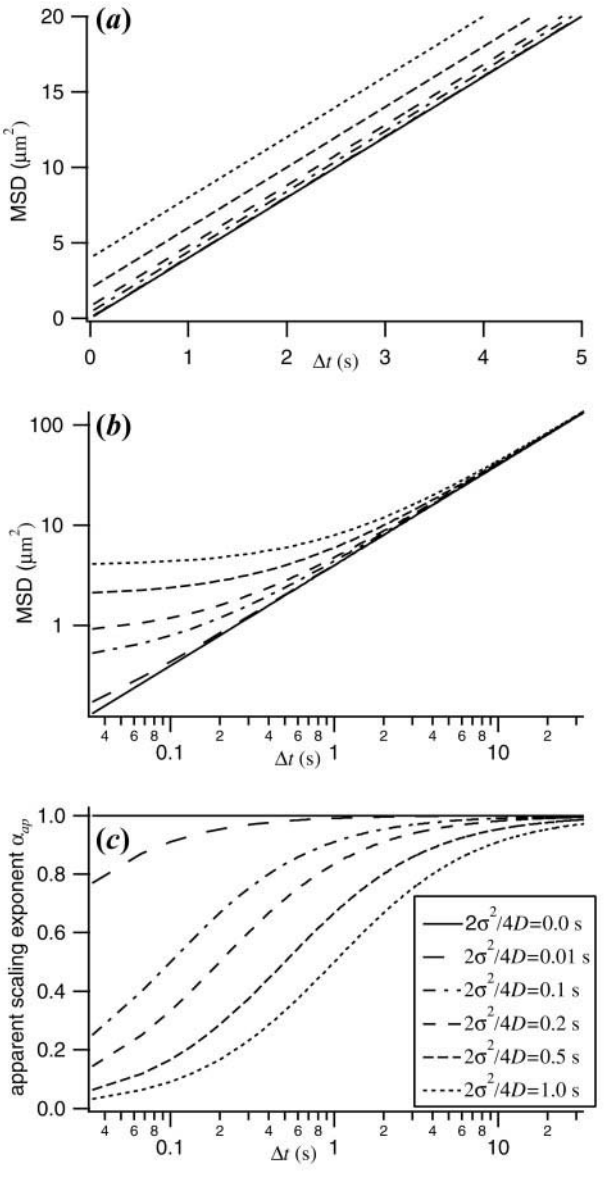

FIGURE 1 A general idea of how error in particle position leads to subdiffusion. (*a*) MSD(Δt), for various error levels, on a linear plot. The solid line is the MSD without noise and the dashed lines are the MSD with noise, MSD_n. The noise results only in a constant offset of the MSD (the range is restricted to highlight the difference between noise levels). (*b*) Logarithmic plot of MSD(Δt). Here, the constant offset due to noise appears large at short times, but small at long times due to the logarithmic scale. Thus, the slope at short times departs significantly from the noise free value leading to apparent subdiffusion. (*c*) $\alpha_{ap}(\Delta t)$, on the same time scale as (*b*). Even small values of $2\sigma 2/4D$ lead to significant reductions in the apparent scaling exponent at short times, whereas larger values can lead to apparent subdiffusion on the order of 10 s.

then approach 1.0 for longer times. This is what causes the apparent subdiffusion of noisy tracks at short times. In addition, Fig. 1 *c* shows how α_{ap} approaches 1.0 for different values of $2\sigma^2/4D$. It should be stressed that this effect will occur for all types of noise in any system using this analysis of the MSD.

METHODS

The experimental procedure used to observe diffusion in lipid monolayers is described in detail elsewhere (Forstner et al., 2001). A lipid monolayer was prepared on a Langmuir trough from vesicles spread from the aqueous subphase, and compressed to the desired surface pressure. The surface pressures used were between 5 and 35 mN/m, the fluid state for the monolayers at about 23°C. The monolayer consisted of DMPC (Avanti Polar Lipids, Alabaster AL) and Texas Red-X labeled dipalmitoyl phosphoethanolamine (DPPE) (Molecular Probes, Eugene, OR) in a molar ratio of 2000:1. At these small molar ratios, there is no phase separation or domain formation. Small gold colloids (30 or 100 nm in diameter) (Goldmark Biologicals, Phillipsburg, NJ) were conjugated with anti-Texas Red-X, and attached to the vesicles before spreading, with a ratio of gold-tagged lipid (DPPE) to untagged lipid (DMPC with DPPE) of ~1:10^9-1:10^{10}. The gold colloids were observed via darkfield microscopy (Olympus BX-FLA, 50 × 0.8 NA darkfield objective, Melville, NY).

The darkfield images were digitized at 30 frames per second, and particles were tracked via the method described by Crocker and Grier (1996) with an accuracy of 100–350 nm. The MSD as a function of time interval Δt is calculated following Qian et al. (1991),

$$\mathrm{MSD}(\Delta t) = \frac{1}{N-n}\sum_{j=1}^{N-n}[\mathbf{r}(j\delta t + n\delta t) - \mathbf{r}(j\delta t)]^2, \qquad (6)$$

where, as in Eq. 1, $\mathbf{r}(t)$ is the position of a particle at time t, δt is the time step between two successive pictures of the labeled molecule, n is the number of steps such that $n\delta t = \Delta t$, and N is the total number of steps in a track. In these experiments, $\delta t = 1/30$ s, and N was up to 10,000 steps. To correct for collective motions of the monolayer, we compared the motions of nearby particles (Forstner et al., 2001).

As described above (Eq. 4), we first find D and σ from a linear fit to the MSD. This proves one method to determine $2\sigma^2/4D$. To find this parameter in a second independent way, we determine the local slope of log(MSD) from d(log(MSD))/d(log(Δt)), which is exactly the apparent scaling coefficient α_{ap} (as α in Eq. 2). The analytic form of this derivative, $\alpha_{ap}(\Delta t) = 1/(1 + 2\sigma^2/4D\Delta t)$, is found in the Appendix (Eq. A10). Finally, we again find $2\sigma^2/4D$ from a one-parameter fit to $\alpha_{ap}(\Delta t)$. It should be noted that the numerical derivative of log(MSD) becomes noisier at long times due to the compression of the logarithmic scale. This is taken into account by weighting the one-parameter fit inversely proportional to the density of the data. We compare the two independently found values of $2\sigma^2/4D$ to test the accuracy of the model.

SIMULATIONS

We run two types of simulations of noisy diffusion. In one, we create artificial noisy movies of particle motion in two dimensions. Our SPT routine is run on these to find the error in particle position as a function of camera noise. In the other, we generate random walks with position error built in. We use these random walks to test our analytic model for apparent subdiffusion.

Error calculation

The standard procedure for estimating errors in particle position in SPT experiments is to attach the particle to a fixed substrate, such as a glass coverslip (Gelles et al., 1988), and track the particle position. Because the particle is fixed, the observed scatter in particle position is the estimate of the error. However, this is an underestimate, due to the enhanced signal-to-noise ratio of a particle fixed to a uniform substrate. For example, the uniform slide reduces the scattering background, enhancing the signal-to-noise ratio for DIC and darkfield microscopy. The same holds true for fluorescence microscopy, because the slide has no fluorescence response. To estimate the error in particle position under experiment-like conditions, we have created simulated movies of a particle diffusing. We first generate random walks following the method described by Saxton (1993), using the probability distribution for the step size r,

$$\mathrm{P}(r) = \frac{1}{4\pi D\delta t}\exp\left[-\frac{r^2}{4D\delta t}\right], \qquad (7)$$

where δt is the time between steps, as above. For each time step δt, the distribution is inverted to calculate a step size based on a uniform random variable [0, 1]. The direction of the step is then picked randomly from $[0, 2\pi]$. For the specific parameters, we use a diffusion coefficient $D = 1 \times 10^{-8}$ cm^2/s and $\delta t = 0.033$ s (similar to DMPC monolayers and video-rate microscopy, respectively).

These random walks are then used as the basis of a simulated movie. We created a particle with a Gaussian profile of the same width we observe via the camera in the real system (~1.5 pixels or 700 nm, full width half maximum). We used intensity profiles and background noise levels representative of real experiments (see Fig. 2). For example, a typical simulation image is shown in Fig. 2 *b*, where the background noise has a Gaussian intensity distribution, with a standard deviation of ~12, and the peak height of the particle is ~60 above the mean background on an 8-bit gray scale (these are the noise and signal values, respectively). The length of the movies is 100–10,000 time steps. To cover the area through which the particle diffuses, the movies are 120 × 120 pixels for the shorter tracks and up to 240 × 240 pixels for longer tracks. We simulate signal-to-noise ratios ranging from 2.5:1 (limit of the tracking routine) to ∞ (no noise).

We then determine the position of the particle in each frame of the simulated movie using the particle-tracking software. These positions are compared with the actual positions of the particle (from the underlying random walk),

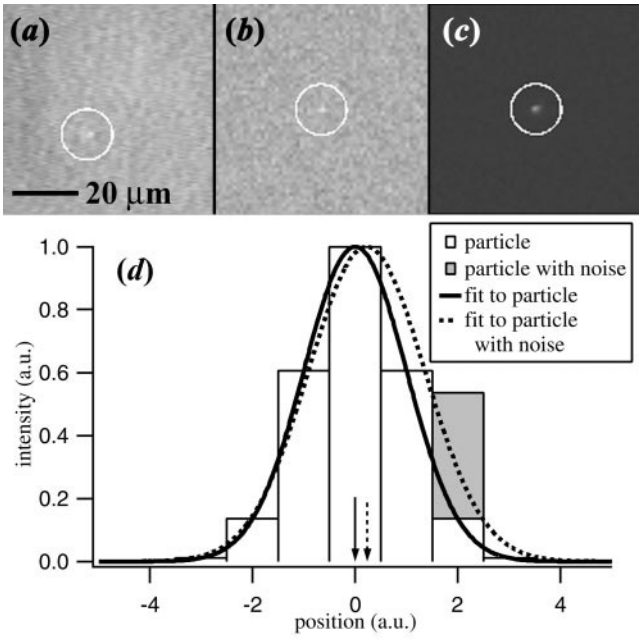

FIGURE 2 Schematic showing how camera noise leads to error in particle position, and how camera noise levels differ between experimental conditions and fixed substrate conditions. (*a*) Real image of a 30-nm gold colloid attached to a monolayer. The white circle is off center due to camera noise. It is deflected left by the slight bright patch to the left of the gold particle. (*b*) Simulated image with similar noise characteristics. Movies of such images are used to track error in particle position. Typical parameters for simulated movies are: background mean intensity of 75–150; particle peak from 30 to 60 above the background; and noise standard deviation of 5–15 around the background, all in 8-bit gray-scale intensities of 0–255. (*c*) Image of a gold colloid dried on a cover slide, the standard method used to estimate error in particle position. The signal-to-noise ratio is a factor of 10 higher than for the center and left images. (*d*) Schematic showing how camera noise leads to error in particle position. The columns indicate pixel intensity. The shaded column represents a higher intensity at that pixel due to camera noise. Gaussian fits to the pixel intensities are shown. The noisy pixel skews the peak toward the right by 0.24 units (*arrows*).

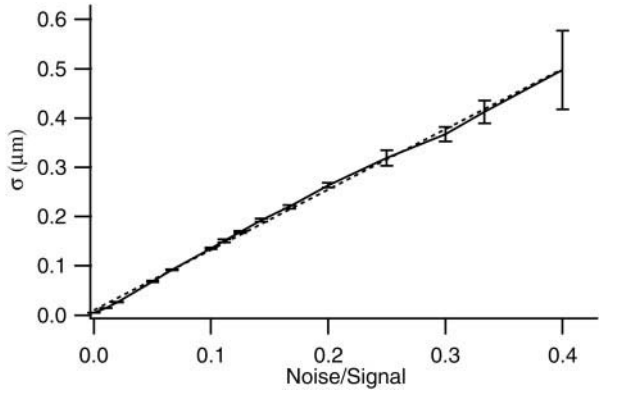

FIGURE 3 Error in particle position as a function of camera noise, calculated from simulated movies. The error in particle position follows a linear relation (*dashed line*) with noise-to-signal ratio (where noise is defined as the standard deviation of the background noise level). For our particular tracking routine, the relationship is $\sigma = 1.22\ \mu\text{m} \times \text{N/S}$. Estimates of error in particle position were made using this formula for the experimental noise-to-signal ratios. This error represented approximately ⅔ of the actual value (see text).

and the average distance σ between actual and calculated particle position is found. A plot of the error σ versus camera noise is shown in Fig. 3. Using the above tracking algorithm and particle width, we find,

$$\sigma = 1.22\ \mu\text{m} \times \text{N/S}, \tag{8}$$

where N/S is the noise-to-signal ratio. However, the specific multiplier depends on the particle width and tracking method used.

Test of analytic model

Simulations were also conducted to test our model of subdiffusion. We again generate random walks based on the probability distribution in Eq. 7, and then add an error to each point based on the distribution (Eq. A2),

$$P(\mathbf{r}, \mathbf{r}') = \frac{1}{2\pi\sigma^2} \exp\left[\frac{|\mathbf{r} - \mathbf{r}|^2}{2\sigma^2}\right], \tag{9}$$

where $\mathbf{r}'$ is the position where the particle is found, and $\mathbf{r}$ is the original position. The simulations conducted above show that the error in particle location can be well fit by such a Gaussian function. Walks of varying length (100–100,000 steps) were created, with $2\sigma^2/4D$ ranging from 0.005 to 0.5 s. We then calculate the MSD from Eq. 6, and follow the technique described above to calculate $\alpha_{ap}(\Delta t)$ and compare this with the underlying parameters σ and D.

RESULTS

The diffusion data from DMPC presented in the section below show both normal and anomalous diffusion. The noise model describes the experimental anomalous diffusion, and is also supported by simulation data. We begin, however, with a test of Eq. 8. To do this, we compare the error in particle position predicted from the camera noise in experimental movies to that found from the experimental mean square displacements.

The value of the error in particle position σ found through the linear fit to the MSD (Eq. 4) accurately predicts the extent of subdiffusion both in experiments and simulations. This error is denoted σ_{fit} below. However, we have also presented two other methods of determining σ. σ_{cam} is the value determined from the signal-to-noise ratio of the actual movies of diffusing particles (Eq. 8). σ_{sim} is the input value for the simulation of noisy random walks (Eq. 9). The ratio $\sigma^2_{cam}/\sigma^2_{fit}$ ranged from -1.7 to 0.84 over 11 experiments,

with σ^2_{fit} even negative for one experiment. If we exclude this experiment, however, the average ratio is 0.64 ± 0.15. Thus, excluding the negative value, camera noise explains about ⅔ of the particle error. The remainder could come from wider variations in image quality during one track, such as spatial and temporal illumination variations within one movie. In contrast, in simulations with σ_{sim} given by Eq. 9, $\sigma_{sim} = \sigma_{fit}$. Thus, the error in particle position accurately propagates through the MSD. Because the value of σ^2_{fit} is the mathematically important quantity, we use it in the subsequent analyses of diffusive tracks, and adopt the notation $\sigma = \sigma_{fit}$.

Diffusion in the homogeneous fluid phase of DMPC monolayers is normal, $\alpha = 1$, and diffusion coefficients D are on the order of 1–10 × 10^{-8} cm^2/s (Cevc, 1993). A typical low camera noise plot of the MSD with time is shown in Fig. 4 *a*, where the offset due to the noise is quite small ($2\sigma^2/4D = 1.6 \times 10^{-2}$ s). Although the motion initially looks subdiffusive ($\alpha_{ap} = 0.8$, Fig. 4, *b* and *c*), it quickly becomes clear that it is normal. The plot of $\alpha_{ap}(\Delta t)$ both from the logarithmic data and linear value of σ and D is given in Fig. 4 *c*. The scaling exponents derived from both methods lie within 0.08, and the difference in $2\sigma^2/4D$ using the two methods is 6×10^{-3} s. The value of $\alpha_{ap}(\Delta t)$ reaches 90% of α within 0.2 s using either method. Thus, for low-noise data, normal diffusion is quickly, though not instantaneously, recovered.

Figure 5 *a* shows a similar plot of the MSD with time for another DMPC monolayer, with higher noise values. In this case, the motion looks very subdiffusive, $\alpha_{ap} = 0.4$ for the first decade (Fig. 5, *b* and *c*). The experimental value of $2\sigma^2/4D = 0.13$ s leads to a predicted time where α_{ap} approaches α of 1.2 s (the actual values are 0.11 and 1.0 s, respectively, see Fig. 5 *c*). Thus, at high noise values, the model accurately predicts both the scaling coefficient and the temporal extent of the apparent subdiffusion.

We use simulated noisy random walks to show that the analytical model gives the correct functional form for the scaling coefficient. Simulations are much faster to conduct than experiments, and so can fill in a much wider range of parameters. To explore the effect of statistics, we calculate α for a variety of track lengths (100–100,000 steps) and noise values. The scaling coefficient for a typical noisy track is shown in Fig. 6 for simulated tracks of 100 and 5000 time points, with a diffusion coefficient D of 1 × 10^{-8} cm^2/s (typical for DMPC monolayers) and an error in particle position σ of 700 nm (higher than the experimental data shown in Fig. 5, but with $2\sigma^2/4D = 0.25$ s). Figure 6 shows the agreement between the analytic form of $\alpha_{ap}(\Delta t)$, and the slope of log(MSD). In addition, the short track (Fig. 6 *b*) shows how difficult it is to determine the scaling exponent in the face of noise with relatively few data.

For simulated tracks of 10,000 steps with the initial value of α_{ap} ranging between 0.06 and 0.87 ($2\sigma^2/4D$ ranging between 0.5 and 0.005 s, respectively), the analytic model

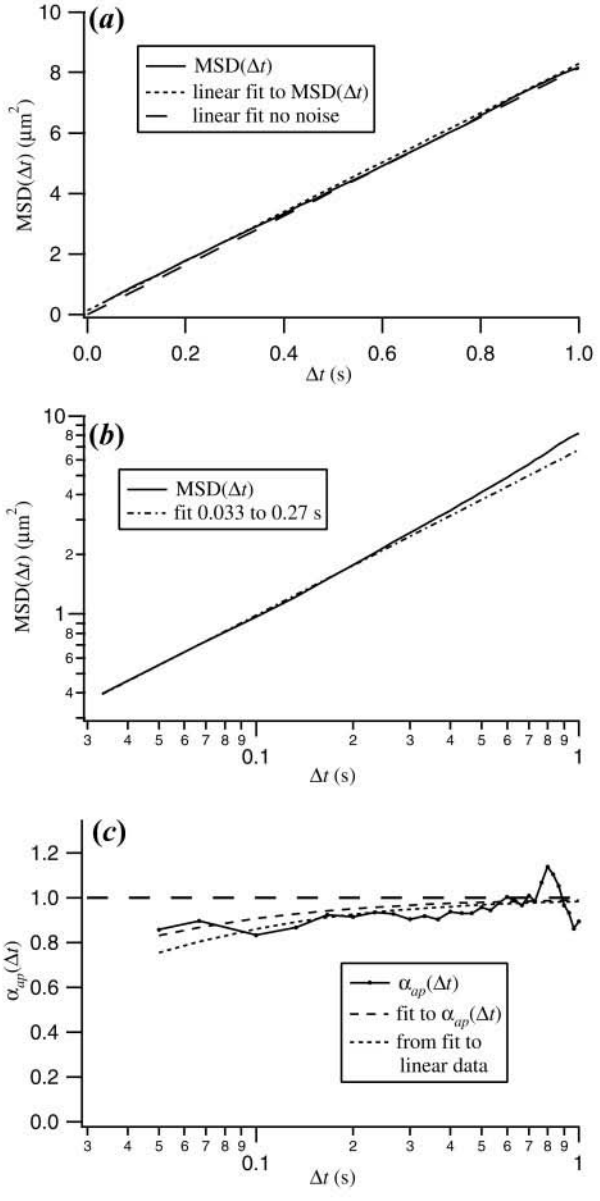

FIGURE 4 Typical data for a low noise experiment, showing the same plots as in Fig. 1. These show that low noise leads to a small offset in the linear MSD, and thus only a small apparent deviation from normal diffusion. (*a*) Linear plot of MSD(Δ*t*). For comparison, the linear fit is shown (*dotted line*), and the linear fit with the noise term, $2\sigma^2$, subtracted out is also shown (*long dashed line*). (*b*) MSD(Δ*t*) in a logarithmic plot. The dashed line is a fit out to 0.27 s, which gives an apparently subdiffusive scaling exponent of 0.8. After ~⅓ s, MSD(Δ*t*) bends upward, and the change in slope is visible. (*c*) $\alpha_{ap}(\Delta t)$, on the same time scale as (*b*). In (*c*), the long dashed line represents the noise-free value of α. The dotted line is $\alpha_{ap}(\Delta t)$ based on the linear fit; the short dashed line is a fit to the experimental $\alpha_{ap}(\Delta t)$ (found from the slope of log(MSD(Δ*t*)), as in Eq. 5). The specific parameters from the experiment are: the total number of steps in this experiment is 2300, at a surface pressure of 15 mN/m. The error in particle position is 120 nm (from Fig. 3), more importantly, σ from the fit is 175 nm. The diffusion coefficient is measured as 1.0 × 10^{-8} cm^2/s.

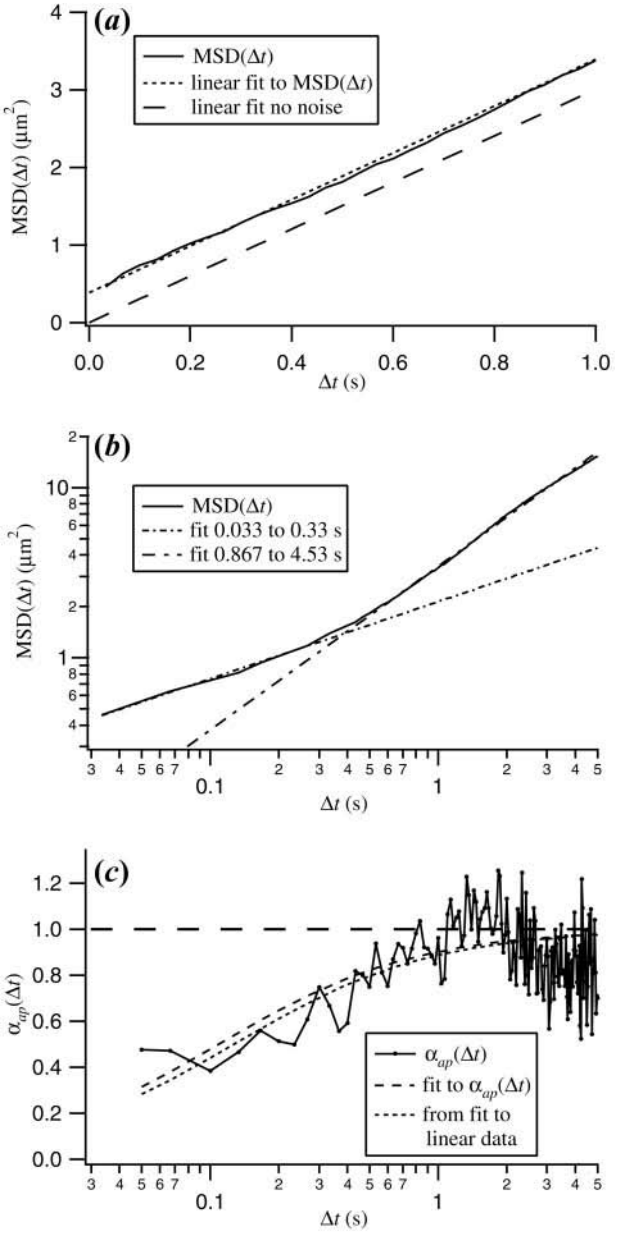

FIGURE 5 Typical high noise experiment, which contrasts with the low noise experiment of Fig. 4. The higher noise values lead to a large offset in the linear MSD, and hence to apparent subdiffusion. (*a*) Linear plot of MSD(Δt). As in Fig. 4, the linear fit (*dotted line*) and linear fit without noise are shown. However, there is a larger offset in this experiment ($2\sigma^2 = 0.38\ \mu m^2$). (*b*) MSD($\Delta t$) on a logarithmic plot. The offset leads to apparently very subdiffusive motion. Over the first decade, a fit to log(MSD(Δt)) gives $\alpha_{ap} = 0.46 \pm 0.06$. At longer times, the MSD returns to normal diffusion, $\alpha_{ap} = 0.96 \pm 0.07$ (*upper* and *lower dashed lines*, respectively). (*c*) $\alpha_{ap}(\Delta t)$ on the same time scale as (*b*); the solid line is the gradient of log(MSD(Δt)). As in Fig. 4, the dotted line is $\alpha_{ap}(\Delta t)$ based on the linear fit, the short dashed line is a fit to the gradient. Once again, $\alpha_{ap}(\Delta t)$ based on the linear fit is a good predictor of the apparent scaling exponent. The specific parameters from the experiment are: the total number of steps in this experiment is 2511, at a surface pressure of 23 mN/m (still in the fluid phase). Here we calculate $\sigma = 310$ nm and $D = 3.7 \times 10^{-9}\ cm^2/s$.

works very well. The average deviation between $2\sigma^2/4D$ found from the linear MSD and $2\sigma^2/4D$ from a fit of $\alpha_{ap}(\Delta t)$ to the gradient of log(MSD) is only 0.0005 ± 0.007 s. This is consistent with no difference in $2\sigma^2/4D$ between the analytic form and the actual fit. In addition, the gradient of log(MSD) is within 0.1 of the analytic form of $\alpha_{ap}(\Delta t)$ out to $\Delta t = 10$ s. Once again, the benefit of long tracks, i.e., long time accuracy of scaling behavior, is made clear.

DISCUSSION

Throughout the experiments on DMPC, the initial scaling behavior ranges from highly subdiffusive to approximately normal. In particular, α_{ap} ranges between 0.08 and 1.17 and so the parameter $2\sigma^2/4D$ ranges between 0.38 s and -5×10^{-3} s, respectively. Despite this widely varying behavior, the analytic model presented for $\alpha_{ap}(\Delta t)$ (and hence apparent subdiffusion) works for the entire experimental range of noise. The average difference between $2\sigma^2/4D$ from the derivative of log(MSD), and from the linear fit to the MSD is only $3.7 \times 10^{-3} \pm 11 \times 10^{-3}$ s, consistent with no deviation. For large values of $2\sigma^2/4D$ (0.1 s), there is only a small relative correction (α_{ap}) approaches the actual scaling exponent (α), and when experimental data can be relied upon for the scaling exponent.

As Fig. 1 and the above results demonstrate, even relatively small amounts of noise can lead to apparently large subdiffusive effects at short times. Two practical methods of determining how subdiffusive a track will appear are shown in Fig. 7. The first is the value of the apparent scaling coefficient α_{ap} as a function of $2\sigma^2/4D$ and Δt, and is shown as a contour plot in Fig. 7 *a*. The second is the time at which α_{ap} approaches within 90% of α. This sets a time scale below which information on the scaling coefficient is inaccurate. A contour plot of this time is shown in Fig. 7 *b*, as a function of σ and D. Figure 7 shows that even small errors such as $\sigma = 10$ nm can lead to $\alpha_{ap} < 0.9$ on cells where diffusion coefficients of proteins are on the order of $10^{-11}\ cm^2/s$.

Adding to the impact of small errors for small diffusion coefficients, the standard method of determining σ can be a significant underestimation. This method observes immobile particles, and calculates σ given $D = 0$ ($MSD = 2\sigma^2$). If these particles are immobilized under the same conditions as the SPT experiments (that is, on the same membrane, with the same lighting), σ should be representative. However, if they are immobilized on a solid substrate, the signal-to-noise ratio can increase significantly. In our immobilized particle experiments, the signal-to-noise ratio increases to ~50:1 (a factor of 4–12 from typical noise levels, see Fig. 2 *c*), and so gives an error in particle position of $\sigma = 25$ nm. Thus, for a diffusion coefficient of $1.0 \times 10^{-8}\ cm^2/s$, the time at which α becomes reliable is expected to be 0.006 s (undetectable) but is actually 0.09–0.8

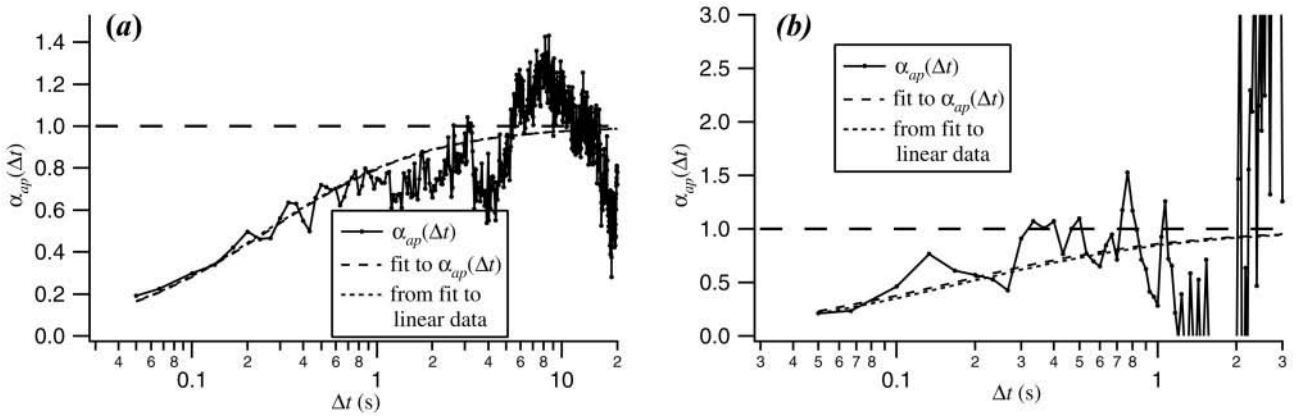

FIGURE 6 The $\alpha_{ap}(\Delta t)$ from simulated noisy random walks, showing both the accuracy of the analytic form and the value of long tracks. (*a*) Walk of 5000 steps, with $2\sigma^2/4D = 0.25$ s. The analytic representation of $\alpha_{ap}(\Delta t)$ (*dashed line*) fits the noisy data (*solid line*) to within ~0.1 out to 5 s. (*b*) Walk of 100 steps, with $2\sigma^2/4D = 0.25$ s. Here, there is a significant variation in $\alpha_{ap}(\Delta t)$. In this case, the scaling exponent has a 0.5 variation about the analytic form after ~0.2 s, showing the difficulty in determining an accurate scaling exponent for short tracks.

s (beyond the first decade). Indeed, this would cause the apparent subdiffusion to be accepted as real.

One clue that noise may be the cause of subdiffusion is a widely varying scaling exponent. The scaling exponent can change based on the underlying model of subdiffusion and parameters in the model, for example, obstacle fraction (Saxton, 1994). However, if lighting conditions differ from experiment to experiment (as they can without affecting the diffusion coefficient), or even from location to location within the same experiment (the sides of cells may be out of focus compared to the top, for example), the value of α_{ap} will vary. Cases such as our DMPC study with widely ranging values of α_{ap} should be considered with particular care to be sure that noise is not a contributing factor to the observation of anomalous diffusion.

The method of determining the scaling coefficient described in this paper assumes underlying normal diffusion. However, even if anomalous diffusion is occurring, the noise effect can skew the calculated α_{ap} to lower values. An analytical formula for α_{ap} requires knowledge of the step size distribution, and, as such, can be quite complex or nonexistent in the anomalous diffusion case. In a first approximation, though, α_{ap} can be found by adding a constant noise term to the MSD (Eq. 1) (approximate because this separation requires a Gaussian step-size distribution). Thus,

$$\alpha_{ap} = \frac{d}{d(\log(\Delta t))}\log(MSD)$$

$$= \frac{d}{d(\log(\Delta t))}\log(4D\Delta t^{\alpha} + 2\sigma^2). \qquad (10)$$

Using a similar method to that in the mathematical appendix, we arrive at,

$$\alpha_{ap} = \alpha\left[\frac{1}{1 + 2\sigma^2/4D\Delta t^{\alpha}}\right], \qquad (11)$$

where α is the actual anomalous diffusion scaling exponent as above. Consequently, the apparent scaling exponent is reduced in a very similar way to that seen in normal diffusion with noise. Finding α from Eq. 11 is difficult because of its appearance in Δt^{α}. Curve fitting with a variable exponent does not converge reliably, and is thus subject to the same constraints that lead to the use of Eq. 2 instead of Eq. 1. The most that can be taken from Eq. 11 is that, once again, a time scale exists below which the scaling coefficient is inaccurate.

The experiments in this study show that subdiffusion results from error in particle position in one specific case, namely that of DMPC monolayers in the fluid (liquid-expanded) phase. In general, though, the result is system independent: apparent subdiffusion arises solely from errors in finding particle position and the analysis of log(MSD) versus log(Δt). Ultimately, error in particle position is inherent to the SPT technique. Typical tracking routines may find particle location by fitting a Gaussian intensity profile to the actual intensity profile of the particle and taking the peak of the Gaussian as the particle position, or by using the weighted center of intensity as the particle position. Either way, if a pixel within the fitting routine is artifactually brighter or dimmer due to noise, the particle position is shifted closer or further from that pixel, respectively (see Fig. 2 *d*). The details of the size of the error depend on the specific tracking routine.

Although the consideration of noise in single-particle tracking is not new (Qian et al., 1991; Dietrich et al., 2002), noise as a cause of apparent subdiffusion was unanticipated. We have suggested one method to circumvent the noise problem: there is a timescale beyond which the impact of camera noise will be negligible. Other analyses may intrinsically circumvent the noise problem, or require other remedies. Additionally, there may be other mathematical ways

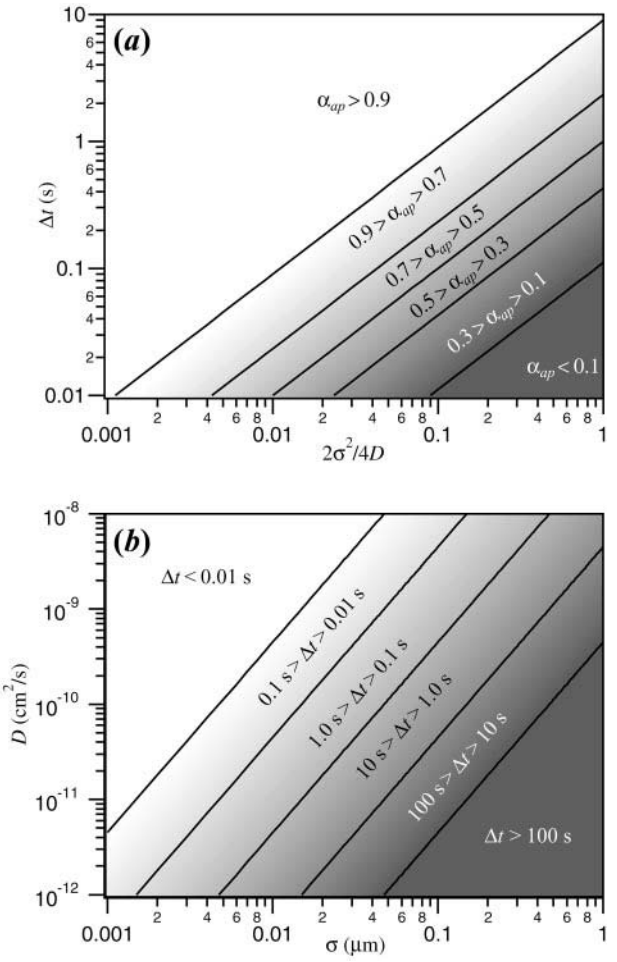

FIGURE 7 Two methods for quickly determining the amount and length of apparent subdiffusion from SPT data. (*a*) α_{ap} as a function of $2\sigma^2/4D$ and Δt. This graph gives the level of apparent subdiffusion for a given error (σ)–diffusion coefficient (D) combination and time length. For example, $2\sigma^2/4D = 0.05$ s corresponds to $\sigma = 10$ nm and $D = 10^{-11}$ cm^2/s or $\sigma = 100$ nm and $D = 10^{-9}$ cm^2/s (two typical combinations). Brownian motion appears subdiffusive out to 0.5 s in this case. (*b*) Time (Δt) at which α_{ap} reaches 0.9 as a function of error and diffusion coefficient. This time can be long (~1 s) for the above values of σ and D, and even longer for marginally noisier data.

to attack the issue. However, the error in particle position itself is inescapable, and should carefully be considered in any SPT experiment.

APPENDIX

One way of describing a two-dimensional random walk is in terms a probability P($\mathbf{r}$, t) of finding a particle at position $\mathbf{r}$ after time t (dropping the symbol Δ), given by,

$$\mathrm{P}(\mathbf{r}, t) = \frac{1}{4\pi Dt}\exp\left[-\frac{r^2}{4Dt}\right], \tag{A1}$$

where D is the diffusion coefficient. The camera noise can be modeled by a probability P($\mathbf{r}$, $\mathbf{r}'$) of detecting the particle at position $\mathbf{r}'$ given that the particle is actually at position $\mathbf{r}$,

$$\mathrm{P}(\mathbf{r}, \mathbf{r}') = \frac{1}{2\pi\sigma^2}\exp\left[-\frac{|\mathbf{r}-\mathbf{r}'|^2}{2\sigma^2}\right], \tag{A2}$$

where σ is the standard deviation of the error in positioning accuracy. We can then combine these probabilities into a new function P$'$($\mathbf{r}'$, t), which gives the probability of finding the particle at $\mathbf{r}'$ at time t, given by,

$$\begin{aligned}\mathrm{P}'(\mathbf{r}', t) &= \int_0^\infty r\,\mathrm{d}r\int_0^{2\pi}\mathrm{d}\theta\mathrm{P}(\mathbf{r}, t)\mathrm{P}(\mathbf{r}, \mathbf{r}')\\ &= \int_0^\infty r\,\mathrm{d}r\int_0^{2\pi} d\theta\,\frac{1}{4\pi Dt}\frac{1}{2\pi\sigma^2}\\ &\quad\times\exp\left[-\frac{r^2}{4Dt}-\frac{|\mathbf{r}-\mathbf{r}'|^2}{2\sigma^2}\right].\end{aligned} \tag{A3}$$

Expanding the exponent in the lower term, we arrive at a new exponent,

$$-\frac{r'^2}{2\sigma^2}-\frac{(2\sigma^2+4Dt)r^2}{2\sigma^2 4Dt}+\frac{2rr'\cos\theta}{2\sigma^2}, \tag{A4}$$

where θ is the angle between the vectors $\mathbf{r}$ and $\mathbf{r}'$. The integral over θ becomes

$$\int_0^{2\pi} d\theta\exp\left[\left(\frac{rr'}{\sigma^2}\right)\cos\theta\right] = 2\pi J_0\left(i\frac{rr'}{\sigma^2}\right), \tag{A5}$$

following Eqs. 9.6.3 and 9.6.16 in Abramowitz and Segun (1965), where J_0 is the Bessel function. The integral over r (independent of prefactors) becomes

$$\begin{aligned}&\int_0^\infty r\,\mathrm{d}r\exp\left[-\frac{2\sigma^2+4Dt}{2\sigma^2 4Dt}r^2\right]J_0\left(\frac{ir'}{\sigma^2}r\right)\\ &\quad=\frac{1}{2}\frac{2\sigma^2 4Dt}{2\sigma^2+4Dt}\exp\left[\frac{4Dt}{2\sigma^2(2\sigma^2+4Dt)}r'^2\right],\end{aligned} \tag{A6}$$

as in Eq. 11.4.29 in Abramowitz and Segun (1965). P$'$($\mathbf{r}'$, t) is thus (Eqs. A3–A6),

$$\begin{aligned}\mathrm{P}'(\mathbf{r}', t) &= \frac{1}{4\pi Dt}\frac{1}{2\pi\sigma^2}2\pi\frac{1}{2}\frac{2\sigma^2 4Dt}{2\sigma^2+4Dt}\\ &\quad\times\exp\left[\left(\frac{4Dt}{2\sigma^2(2\sigma^2+4Dt)}-\frac{1}{2\sigma^2}\right)r'^2\right]\\ &= \frac{1}{\pi(2\sigma^2+4Dt)}\exp\left[-\frac{r'^2}{2\sigma^2+4Dt}\right].\end{aligned} \tag{A7}$$

The mean squared displacement then becomes

$$\begin{aligned}\mathrm{MSD} &= \langle \mathbf{r}'^2 \rangle \\ &= \int_0^\infty 2\pi r'\, \mathrm{d}r' r'^2 \frac{1}{\pi(2\sigma^2 + 4Dt)} \exp\left[\frac{-r'^2}{2\sigma^2 + 4Dt}\right] \\ &= 2\sigma^2 + 4Dt. \end{aligned} \tag{A8}$$

Thus, the effect of an error σ in particle location is to add a constant to the mean square displacement (as in Eq. 4 in the main text).

To describe what occurs in the presence of noise, where $\langle \mathbf{r}^2 \rangle = 4Dt + 2\sigma^2$ (from Eq. 4 or Eq. A8), we consider the plot of log(MSD) versus log(t). The slope of this plot is α_{ap}, from MSD $\sim t^\alpha$. The slope is given by

$$\alpha_{\mathrm{ap}}(t) = \frac{\mathrm{d}(\log(\mathrm{MSD}))}{\mathrm{d}(\log(t))} = \frac{\mathrm{d}}{\mathrm{d}(\log(t))}\left[\log(4Dt + 2\sigma^2)\right]. \tag{A9}$$

Substituting $t = 10^x$, we arrive at,

$$\begin{aligned}\alpha_{\mathrm{ap}}(t) &= \frac{\mathrm{d}}{\mathrm{d}x}\left[\log(4D(10^x) + 2\sigma^2)\right] \\ &= \frac{\ln(10)\log(e)4D(10^x)}{4D(10^x) + 2\sigma^2} \\ &= \frac{4Dt}{4Dt + 2\sigma^2} \\ &= \frac{1}{1 + (2\sigma^2/4Dt)}. \end{aligned} \tag{A10}$$

The authors would like to thank Dr. J. B. Swift and Dr. M. S. Martin for instructive conversations.

This work was supported by the Texas Advanced Research Program under grant number 003658-0429-1999.

REFERENCES

Abramowitz, M., and I. A. Segun, editors. 1965. Handbook of Mathematical Functions. Dover Publications, New York.

Anderson, C. M., G. N. Georgiou, I. E. Morrison, G. V. Stevenson, and R. J. Cherry. 1992. Tracking of cell surface receptors by fluorescence digital imaging microscopy using a charge-coupled device camera. Low-density lipoprotein and influenza virus receptor mobility at 4 degrees C. *J. Cell Sci.* 101:415–425.

Cevc, G., editor. 1993. Phospholipids Handbook. Marcel Dekker, New York. 464.

Cherry, R. J., P. R. Smith, I. E. Morrison, and N. Fernandez. 1998. Mobility of cell surface receptors: a re-evaluation. *FEBS Lett.* 430: 88–91.

Collier, I. E., S. Saffarian, B. L. Marmer, E. L. Elson, and G. Goldberg. 2001. Substrate recognition by gelatinase A: the C-terminal domain facilitates surface diffusion. *Biophys. J.* 81:2370–2377.

Crocker, J. C., and D. G. Grier. 1996. Methods of digital video microscopy for colloidal studies. *J. Colloid Interface Sci.* 179:298–310.

Dietrich, C., B. Yang, T. Fujiwara, A. Kusumi, and K. Jacobson. 2002. Relationship of lipid rafts to transient confinement zones detected by single particle tracking. *Biophys. J.* 82:274–284.

Feder, T. J., I. Brust-Mascher, J. P. Slattery, B. Baird, and W. W. Webb. 1996. Constrained diffusion or immobile fraction on cell surfaces: a new interpretation. *Biophys. J.* 70:2767–2773.

Forstner, M. B., J. Käs, and D. Martin. 2001. Single lipid diffusion in Langmuir monolayers. *Langmuir.* 17:567–570.

Gelles, J., B. J. Schnapp, and M. P. Sheetz. 1988. Tracking kinesin-driven movements with nanometre-scale precision. *Nature.* 331:450–453.

Ghosh, R. N., and W. W. Webb. 1994. Automated detection and tracking of individual and clustered cell surface low density lipoprotein receptor molecules. *Biophys. J.* 66:1301–1318.

Jacobson, K., E. D. Sheets, and R. Simson. 1995. Revisiting the fluid mosaic model of membranes. *Science.* 268:1441–1442.

Kusumi, A., Y. Sako, and M. Yamamoto. 1993. Confined lateral diffusion of membrane receptors as studied by single particle tracking (nanovid microscopy). Effects of calcium-induced differentiation in cultured epithelial cells. *Biophys. J.* 65:2021–2040.

Lee, G. M., A. Ishihara, and K. A. Jacobson. 1991. Direct observation of Brownian motion of lipids in a membrane. *Proc. Natl. Acad. Sci. U.S.A.* 88:6274–6278.

Qian, H., M. P. Sheetz, and E. L. Elson. 1991. Single particle tracking. Analysis of diffusion and flow in two-dimensional systems. *Biophys. J.* 60:910–921.

Saxton, M. J. 1993. Lateral diffusion in an archipelago. Single-particle diffusion. *Biophys. J.* 64:1766–1780.

Saxton, M. J. 1994. Anomalous diffusion due to obstacles: a Monte Carlo study. *Biophys. J.* 66:394–401.

Saxton, M. J. 1995. Single-particle tracking: effects of corrals. *Biophys. J.* 69:389–398.

Saxton, M. J. 1996. Anomalous diffusion due to binding: a Monte Carlo study. *Biophys. J.* 70:1250–1262.

Saxton, M. J., and K. Jacobson. 1997. Single-particle tracking: applications to membrane dynamics. *Annu. Rev. Biophys. Biomol. Struct.* 26: 373–399.

Schütz, G. J., G. Kada, V. P. Pastushenko, and H. Schindler. 2000. Properties of lipid microdomains in a muscle cell membrane visualized by single molecule microscopy. *EMBO J.* 19:892–901.

Schütz, G. J., H. Schindler, and T. Schmidt. 1997. Single-molecule microscopy on model membranes reveals anomalous diffusion. *Biophys. J.* 73:1073–1080.

Sheetz, M. P., S. Turney, H. Qian, and E. L. Elson. 1989. Nanometre-level analysis demonstrates that lipid flow does not drive membrane glycoprotein movements. *Nature.* 340:284–288.

Smith, P. R., I. E. Morrison, K. M. Wilson, N. Fernandez, and R. J. Cherry. 1999. Anomalous diffusion of major histocompatibility complex class I molecules on HeLa cells determined by single particle tracking. *Biophys. J.* 76:3331–3344.